JOURNAL OF APPLIED ELECTROCHEMISTRY **28** (1998) 1095–1099

Crystallographic textures and magnetic properties of electroformed nickel

K. C. CHAN, N. S. QU

Department of Manufacturing Engineering, The Hong Kong Polytechnic University, Hong Kong

D. ZHU

Department of Mechanical Engineering, Nanjing University of Aeronautics & Astronautics, Nanjing, China

Received 10 September 1997; accepted in revised form 9 February 1998

The magnetic properties of nickel deposits are known to be related to their crystallographic textures. Although there has been significant work investigating the relationship between crystallographic textures and magnetic properties of sputtered ferro-magnetic films, relatively less effort has been spent on studying electroformed nickels. Orientation distribution functions and coercivity of the nickel deposits, electroformed by using a nickel sulphamate bath and pulse-reverse currents, have been determined and their relationship examined. It was found that the [1 0 0] fibre texture with different orientation densities was formed at different on-times and off-times, and that at the same deposition thickness the coercivity increased with increase in the orientation density of the [1 0 0] fibre texture. This findings are of high significance as they can serve as guidelines for the production of nickel deposits with defined magnetic properties through the control of crystallographic texture by varying the pulse parameters in pulse-reverse current electroforming.

Keywords: *crystallographic texture*, *electroforming*, *magnetic properties*, *nickels*, *pulse-reverse current*

1. Introduction

In the past decade, the development of micromagnetic actuators for micromachines by electroforming has aroused much interest in studying the magnetic properties of electrodeposited ferromagnetic materials such as nickel [1–3]. Since the magnetic properties are known to be related to the crystallographic textures, much research effort has also been spent in investigating crystallographic textures in the nickel electrodeposition process. The crystallographic texture of nickel deposits is dependent on electrolysis conditions and electrolyte compositions [4, 5], also a fibre texture along the electric field direction was observed. With direct current, four kinds of texture (i.e., orientations [1 0 0], [1 1 0], [2 1 0] and [2 1 1]) are observed in the deposits under different conditions. The electrocrystallization of nickel is known to be a highly inhibited process [6, 7]. The textural organization of the deposits has been attributed to the existence or formation of different chemical species in the metal–electrolyte interface (catholyte) during the cathodic process; these are selectively adsorbed on the continually renewed metal surface [8]. With the application of pulse current techniques in nickel electrodeposition, some new parameters are introduced, which influence the electrocrystallization mechanisms and the absorption–desorption phenomena occurring on the metallic surface [9, 10]. The perturbation effect on the crystal growth process is even stronger when pulse reverse current is employed, which is mainly caused by the dissolution of metal during the reversal of the cell polarity [11–14]. However, most of the current analyses are semi-quantitative and have only been performed using a Watts-type bath which is commonly used for decorative industrial applications. Recently, the present authors have successfully carried out quantitative analysis of crystallographic texture in pulse reverse current electroforming of nickel using a sulphamate bath which is more common for microcomponents. The present work aims to further examine the relationship between the crystallographic textures and the magnetic properties of nickel deposits.

2. Experimental details

The bath composition is nickel sulphamate 330 g dm^{-3}; nickel chloride 15 g dm^{-3}; boric acid 30 g dm^{-3} and sodium dodecyl sulphate 0.2 g dm^{-3}. In the electrodeposition process, the electrolyte was gently agitated using a magnetic stirrer, and the temperature was kept at 50 $\pm$ 1 °C. The initial pH of the electrolyte was 4.2, a typical pH value used in electroforming. The waveform of pulse reverse current is shown in Fig. 1, and is defined by the positive peak current density, i_p, the negative peak current density, i_n, the frequency, f, and the duty cycle $T_{on}/(T_{off} + T_{on})$. In the experiments, the deposition time, T_{on}, was varied from 1.2 to 5 ms at a constant off-

0021-891X

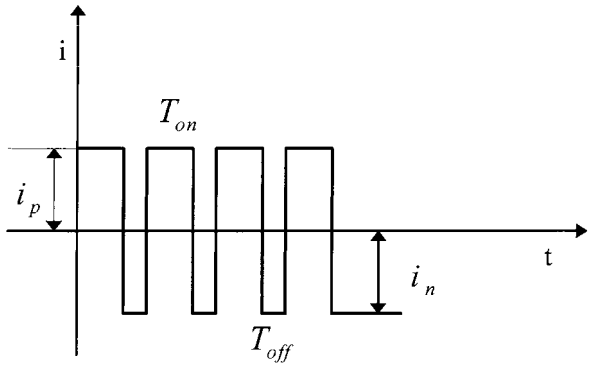

Fig. 1. Waveform of a pulse reverse current.

time of 0.5 ms, and the dissolution time, T_{off}, was varied from 0.5 to 2.0 ms at a constant on-time of 5.0 ms. Both the positive peak current density (i_p) and the negative peak current density (i_n) were 24 A dm^{-2}.

Flat stainless steel mandrels with dimensions of 100 mm × 30 mm × 1 mm were used. Before deposition, they were ground using 400, 800 and 1200 graded emery papers so as to limit the epitaxial influence on the deposit quality. Before applying pulse reverse current, a direct current was first applied for a minute to prevent the mandrel from dissolving. The thickness of the deposition layer of all the samples was 50 ± 0.2 μm which is thick enough to attain a steady-state crystal growth condition [14]. The texture of the nickel deposits were measured by a Philips X-ray diffractometer. Three incomplete pole figures: (110), (200) and (211) (with $0° < \psi < 70°$, $0° < \phi < 90°$) were obtained by the back reflection method at 5° increments using CuK_α radiation. From the pole figures, orientation distribution functions (ODFs) were calculated by the software developed by Cai and Lee using the series expansion method [15]. The coercivity was measured by a vibration sample magnetometer.

3. Results

3.1. *Crystallographic textures and coercivity at a constant on-time*

The ODFs of the electroformed nickels at an on-time of 5.0 ms and at off-times of 0.5, 0.8, 1.0, 1.5 and 2.0 ms were determined and two typical examples are shown in Fig. 2(a) and (b). Based on the ODFs, the orientation densities of the texture components are summarized in Table 1. Although similar textures ([100] fibre texture) are observed at different off-times, the orientation density of the fibre texture is different at different off-times, as shown in Table 1. The effect of off-time on the density of the fibre texture is shown in Fig. 3. The density of the [100] texture is shown to decrease when the off-time increases from 0.5 to 0.8 ms. The density then goes up when the off-time increases from 0.8 to 2.0 ms. The lowest density was found to occur at an off-time of 0.8 ms. Figure 4 shows the effect of off-time on the coercivity of electroforming nickel at a constant on-time of 5.0 ms. The coercivity is shown to decrease when the off-time increases from 0.5 to 0.8 ms. The coercivity then goes up when the off-time increases from 0.8 ms to 2.0 ms. The lowest coercivity was found to occur at an off-time of 0.8. When comparing Fig. 3 with Fig. 4, the general trends of the curves are found to be in reasonable agreement.

3.2. *Crystallographic textures and coercivity at a constant off-time*

The ODFs of the electroformed nickels at on-times of 1.2, 2.0, 3.0, 4.0 and 5.0 ms and at an off-time of 0.5 ms were determined, and two typical examples of these are shown in Fig. 5(a) and (b). Based on the ODFs, the orientation densities of the texture components are summarized in Table 2. Although similar

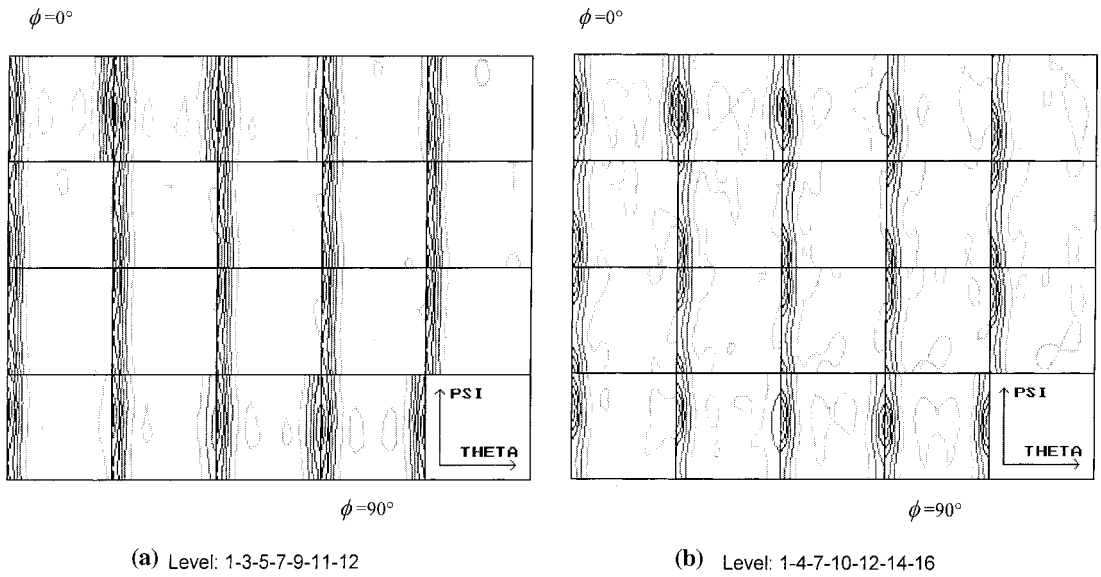

Fig. 2. ϕ-Sections ($\Delta\phi = 5°$) of the ODF of the electroformed nickel formed at an on-time of 5.0 ms and at an off-time of (a) 0.8 ms (b) 2.0 ms.

Table 1. Main texture components of the electroformed nickel formed at a constant on-time of 5 ms and at different off-times

Off-time/ms	*Components*	*Orientation density*
0.5	fibre texture {100}	15.30
	{221}⟨562⟩	1.11
0.8	fibre texture {100}	12.82
	{530}⟨354⟩	1.28
	{552}⟨115⟩	1.36
1.0	fibre texture {100}	13.11
	{120}⟨212⟩	1.84
	{210}⟨001⟩	1.83
	{101}⟨111⟩	1.39
1.5	fibre texture {100}	16.31
	{530}⟨357⟩	1.88
	{113}⟨121⟩	1.75
2.0	fibre texture {100}	16.38
	{120}⟨212⟩	2.01
	{552}⟨115⟩	1.97
	{552}⟨110⟩	1.67

textures ([1 0 0] fibre texture) are also observed at different on-times, the orientation density of the fiber texture is different at different on-times, as shown in Table 2. The effect of on-time on the density of fibre texture is shown in Fig. 6. The density of the [1 0 0] texture is increases when the on-time increases from 1.2 to 3.0 ms. The density then decreases as the on-time increases from 3.0 to 5.0 ms. The highest density is found to occur at an on-time of 3.0 ms. Figure 7 shows the effect of on-time on the coercivity of electroforming nickel at a constant off-time of 0.5 ms. The coercivity increases when the on-time increases from 1.2 to 3.0 ms. The density then decreases as the on-time increases from 3.0 to 5.0 ms. The highest density was found at an on-time of 3.0 ms. Similar to the findings in section 3.1, the general trends of the curves in Fig. 6 and Fig. 7 are also in agreement, although a larger discrepancy is observed.

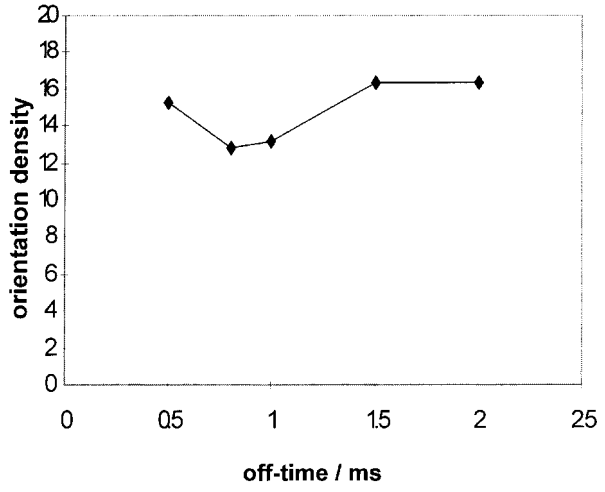

Fig. 3. Orientation density of the [1 0 0] texture of the electroformed nickel formed at a constant on-time of 5.0 ms and at different off-times.

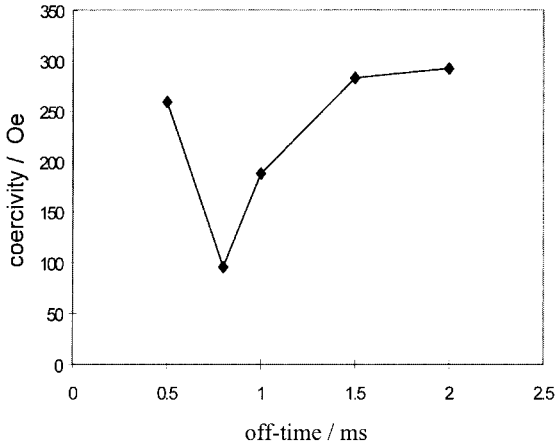

Fig. 4. Coercivity of the electroformed nickel formed at a constant on-time of 5.0 ms and at different off-times.

4. Discussions

4.1. *Effect of off-time on crystallographic texture*

As discussed in [8], the change in density of the [1 0 0] texture in nickel deposits is attributed to the change in the amount of inhibiting chemical species under different conditions. During the on-time, both nickel hydroxide and hydrogen are formed and partially absorbed onto the cathode surface; this inhibits crystal growth. However, in the present experiments, since the longest on-time is 5.0 ms, which is not long enough to allow substantial amount of chemical species to be absorbed onto the cathode surface to inhibit crystal growth, similar [1 0 0] fibre textures are observed in the ODFs. During the off-time, the cathode dissolves because of polarity reversal which results in an increase in the amount of nickel ions and nickel hydroxide near the cathode [8]. As a result, during the on-time, a larger amount of nickel hydroxide is absorbed on the cathode surface, and the amount of nickel deposited increases. In fact, the change of orientation density is considered to be attributed to these two opposing factors. The former one, which inhibits crystal growth, leads to a decrease in orientation density of [1 0 0] fibre texture, whereas the latter factor is advantageous to the formation of [1 0 0] fibre texture. Figure 3 shows that the density of the [100] texture decreases as off-time increases from 0.5 to 0.8 ms, and the density goes up when the off-time increases from 0.8 to 2.0 ms. It is believed that for a fixed on time of 5 ms, when the off-time is shorter than 0.8 ms, the effect of the former factor is larger than that of the latter, the orientation density of the [1 0 0] texture will hence decrease with increasing off-time. On the other hand, when the off-time is above 0.8 ms, the effect of the increase in the nickel deposition rate becomes dominant, which results in an increase in the density of the [1 0 0] texture with increasing off-time. In fact, during the on-time, some other minor texture components such as {2 1 0}, {5 3 0} and {1 1 0} are formed. It has been reported that the formation of these textures is due to the

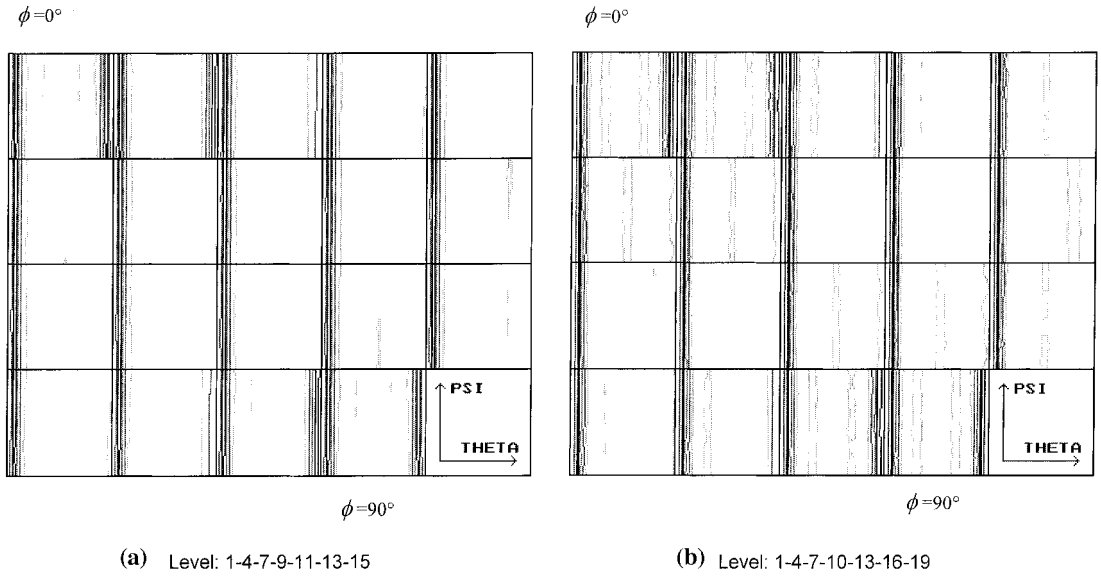

Fig. 5. ϕ-Sections ($\Delta\phi = 5°$) of the ODF of the electroformed nickel formed at an off-time of 5.0 ms and at an on-time of (a) 5.0 ms and (b) 3.0 ms.

presence of nickel hydroxide and hydrogen being absorbed on the cathode surface [7].

4.2. *Effect of on-time on crystallographic texture*

At a constant off-time, an increase in on-time is shown to affect the amount of nickel hydroxide and hydrogen, but to have little effect on the deposition rate during on-time. At the metal–cathode interface, the nickel hydroxide, which is usually produced during off-time, is ionized as follows:

$$Ni(OH)_2 = Ni^{2+} + 2\,OH^-$$

and OH^- migrates towards the anode. The amount of nickel hydroxide is therefore reduced. On the other hand, the amount of hydrogen increases with increasing on-time [8]. The change in orientation density is therefore related to these two competing factors. It is believed that when the on-time is less than 3.0 ms, the effect of the decrease in the amount of nickel hydroxide absorbed on the cathode surface is larger than that of the increase in the amount of hydrogen. The orientation density of the [100] fibre texture therefore increases with increasing on-time. However, when the on-time is above 3.0 ms, the increases in hydrogen plays a more important role in inhibiting crystal growth and the orientation density of the [1 0 0] fibre texture decreases with increasing on-time.

Table 2. Main texture components of the electroformed nickel formed at a constant off-time of 0.5 ms and at different on-times

On-time/ms	*Components*	*Orientation density*
1.2	fibre texture {100}	16.60
	{201}⟨142⟩	2.22
	{122}⟨641⟩	3.47
	{110}⟨112⟩	2.79
	{113}⟨110⟩	4.48
	{210}⟨120⟩	1.86
2.0	fibre texture {100}	18.60
	{305}⟨573⟩	1.88
3.0	fibre texture {100}	19.63
	{530}⟨351⟩	1.42
	{102}⟨221⟩	1.54
4.0	fibre texture {100}	18.65
	{407}⟨734⟩	1.18
5.0	fibre texture{100}	15.30
	{221}⟨562⟩	1.11

4.3. *Relationship between crystallographic texture and coercivity*

To illustrate better the relationship between coercivity and crystallographic textures of electroformed nickel, a coercivity against orientation density of the [1 0 0] texture curve was further constructed and is shown in Fig. 8. It was found that the coercivity

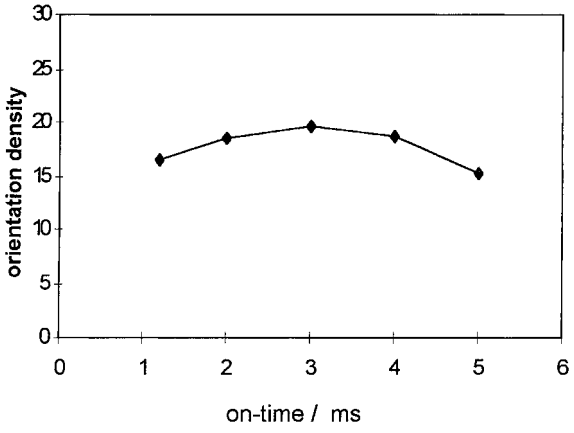

Fig. 6. Orientation density of the [1 0 0] texture of the electroformed nickel formed at a constant off-time of 0.5 ms and at different on-times.

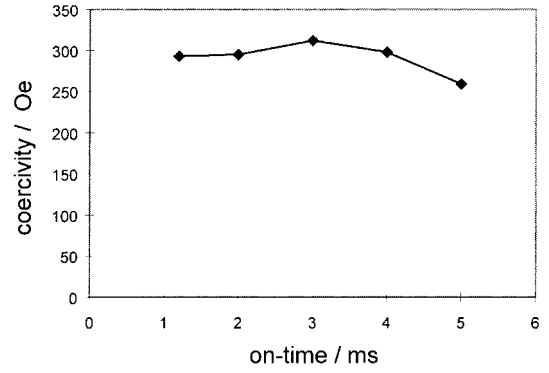

Fig. 7. Coercivity of the electroformed nickel formed at a constant off-time of 0.5 ms and at different on-times.

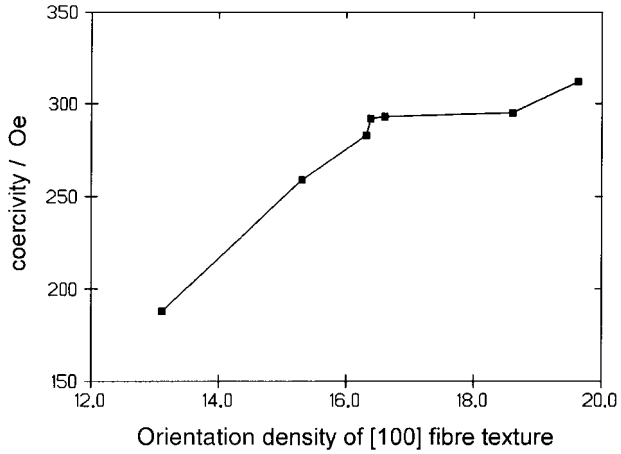

Fig. 8. Relationship between orientation density of the [1 0 0] textures and coercivity of the electroformed nickel.

increases with the increase in the density of the [1 0 0] fibre texture at the same deposition thickness. This finding is of high significance as it is now more feasible to produce a nickel deposit with a defined magnetic property through the control of the crystallographic texture. However, in the present analysis, the spread of the fibre texture and the effect of minor texture components have not been taken into consideration, which may explain the discrepancies observed in the results.

5. Conclusions

Different orientation densities of the [1 0 0] fibre texture were observed at different on-times and off-times. The change in orientation density of the [1 0 0] fibre texture is considered to be related to the change in the amount of inhibiting chemical species. In general, the measured coercivity is found to increase with increase in orientation density of the [1 0 0] fibre texture at the same deposition thickness. It is considered that the spread of the fibre texture and the effect of minor texture components have to be taken into consideration so that their relationship can be better understood.

Acknowledgement

Financial support from The Hong Kong Polytechnic University is duly acknowledged.

References

[1] H. Lehr, W. Ehrfeld, M. Schmidt, E. Kallenbach and H. A. Tuan, *J. Micromech. Microeng.* **2** (1992) 229.
[2] H. Guckel, K. J. Skrobis, T. R. Christenson, J. Klein, S. Han, B. Choi, E. G. Lovell and T. W. Chapman, *Journal of Micromechanics and Microengineering*, Vol 1, 1991, p. 135.
[3] S. C. Terry, J. H. Jerman and J. B. Angell, *IEEE Trans. Electron Devices* **26** (1979) 1180.
[4] W. Paatsch, *Plat. Surf. Finish.* **75** (1988) 52.
[5] J. Amblard, M. Froment, G. Maurin and N. Spyrellis, Proceedings of the 170th meeting of the Electrochemical Society, San Diego, CA (1986), Ext. Abstr. 469, p. 700.
[6] C. Kollia, Z. Loizos and N. Spyrellis, *Surf. Coat. Technol.* **45** (1991) 155.
[7] J. Amblard, I. Epelboin, M. Froment and G. Maurin, *J. Appl. Electrochem.* **9** (1979) 233.
[8] C. Kollia and N. Spyrellis, *Surf. Coat. Technol.* **57** (1993) 71.
[9] N. Ibl, J. C. Puipe and H. Angerer, *Surf. Technol.* **6** (1978) 287.
[10] N. Ibl, *Surf. Coat. Technol.* **10** (1980) 81.
[11] C. Kollia, N. Spyrellis, J. Amblard, I. Epelboin, M. Froment and G. Maurin, *J. Appl. Electrochem.* **20** (1990) 1025.
[12] C. Kollia and N. Spyrellis, in 'Advanced Materials and Processes', Vol. 2 (edited by H. E. Exner and V. Schumacher), DGM, Oberursel, Germany (1990), p. 1151.
[13] C. Kollia and N. Spyrellis, Proceedings of the 2nd European Conference on Advanced Materials and Processes, Cambridge, London (1991), p. 71.
[14] O. Teschke and D. Menez Soares, *J. Electrochem. Soc.* **130**(2) (1983) 308.
[15] M. J. Cai and W. B. Lee, *J. Materi. Process. Technol.* **48** (1995) 51.